PERGAMON

International Journal of Heat and Mass Transfer 43 (2000) 1999–2008

International Journal of HEAT and MASS TRANSFER

www.elsevier.com/locate/ijhmt

Pool boiling CHF on a laser heated thin plate

Henrik Gjerkeš, Iztok Golobič*

Faculty of Mechanical Engineering, University of Ljubljana, Aškerčeva 6, 1000 Ljubljana, Slovenia

Received 7 May 1999; received in revised form 21 July 1999

Abstract

The technique of laser heating a thin metal foil was used to experimentally observe local phenomena in pool boiling CHF on a small flat surface. The experiments were performed with saturated water boiling on 25 μm thick copper and titanium foils with heating surface diameters ranging from 2.27 to 9 mm. The number of simultaneously active nucleation sites depends on the heat flux and the size and material of the laser heated surface. A reduction in the heating surface diameter D_H moves the transition between one and several simultaneously active nucleation sites towards higher heat fluxes. CHF for small heating surfaces is lower than that for entirely heated surfaces. The variation of the ratio of bubble/vapour mass diameter to the heating surface diameter, D_B/D_H, with D_H is similar to the variation of CHF with D_H. CHF is significantly influenced by the number of simultaneously active nucleation sites. The influence of heating of the surrounding surface on decreasing D_H, which was observed using two laser beams with different diameters was more intense at higher D_H on Cu foil than on Ti foil.

Keywords: Boiling; Heat transfer; Nucleonics

1. Introduction

Critical heat flux (CHF) is a complex phenomenon and involves many aspects that still require clarification. CHF analyses are based primarily on experiments conducted using small electric heaters [1–5]. Additional research focusing on local observations of the processes involved in CHF will need to be conducted in order to better understand this phenomenon [6–8]. Even though such experiments on small heating surfaces have several shortcomings, they provide a better and more detailed insight into the boiling process.

Although a significant progress has been made in the study of CHF, a mechanistic model which would be able to describe and to predict the pool boiling CHF on a small horizontal surface has not been developed. CHF is not an isolated phenomenon, but a continuation of nucleate boiling [9]. The study of spatio-temporal behaviour of the wall superheat in the vicinity of nucleation sites and its consequences for instantaneous heat flux can be found for both low heat flux boiling [10–12] and high heat flux boiling [13]. In order to gain a deeper insight into the processes taking place in pool boiling, which will enable an appropriate data input to the predicting methods for the practical engineer, further development of experimental methods for the measurement of local and spatial instantaneous characteristics on a boiling surface is necessary [14,15].

The measurements of Katto and Otokuni [16] shows that CHF in pool boiling is not likely to be a phenomenon created by the instability or any other limiting

* Corresponding author. Tel.: +386-61-1771-420; fax: +386-61-218-567.

E-mail address: iztok.golobic@uni-lj.si (I. Golobič).

0017-9310/00/$ - see front matter
PII: S0017-9310(99)00263-X

Nomenclature

$\mathscr{A}$	diffusive absorptivity
D_B	bubble or vapour mass departure diameter (m)
D_H	heating area diameter (m)
$D_{H,\infty}$	heated surrounding area diameter (m)
f	bubble or vapour mass frequency (s^{-1})
q'_{1-2}	maximum heat flux for a given D_H at which only one nucleation centre is active (W m^{-2})
q''_{1-2}	minimum heat flux for a given D_H at which several nucleation centres are active simultaneously (W m^{-2})
q_{CHF}	critical heat flux (W m^{-2})
q_H	heat flux in heating area (W m^{-2})
$q_{H,\infty}$	heat flux in heated surrounding area (W m^{-2})
P	laser beam power (W)
R^2	coefficient of determination
r_A	arithmetic mean roughness (μm)

condition of the escaping vapour flow. On the other hand there is no satisfactory explanation for a strong increase in CHF in pool boiling on an enhanced heat transfer surface, on which CHF was obtained up to a factor of 3 greater than on the basic surface [17]. We believe that the key to understanding CHF is in the interaction between heater side parameters, the heater–fluid interface parameters and fluid side parameters. Identification of the various influential parameters involved in CHF and their interaction requires future experimental efforts, especially toward local observation of the phenomena, which are possible with the controlled nucleation sites system [15,18].

This paper presents experimental work, which was performed to determine the CHF and to study the local parameters influencing CHF on a small heating surface.

2. Experimental device

The test vessel (Fig. 1) contains saturated water at atmospheric pressure. It is constructed of stainless steel with a thickness of 2 mm and has the shape of a horizontal cylinder with a diameter of 200 mm and a length of 200 mm. The cylinder is closed at both ends with 5 mm thick plates of borosilicate glass. The test vessel contains an electric immersion heater (2) with a power of 1.5 kW and a copper tube condenser (3). A glass condenser (4) is located externally to the vessel. Heat losses through the cylinder wall were compensated for by an electric heater on its circumference with a maximum power of 1.5 kW which was regulated by a variac. The electric heater on the circumference is insulated with glass wool and covered with aluminium foil.

At the bottom of the vessel, a test section (1) with metal foil was located which was in contact with the water on the upper side, while the lower side was irradiated by laser beams. A thin metal foil was mechanically attached and sealed with silicon putty.

As a heat source a continuous wave Nd:YAG laser with a wavelength of 1064 nm and a maximum power of 70 W was used. The laser beam passed through a plano-convex lens (I). Using a polarising beamsplitter cube (II) it was divided into two differently polarised beams (A and B) of approximately equal power at an angle of 90°. Polarisation was necessary due to the use of variable attenuators, which were used to set the power of each individual beam separately. After exiting from the attenuators, the path of the two beams to the test section was determined by the position of mirrors

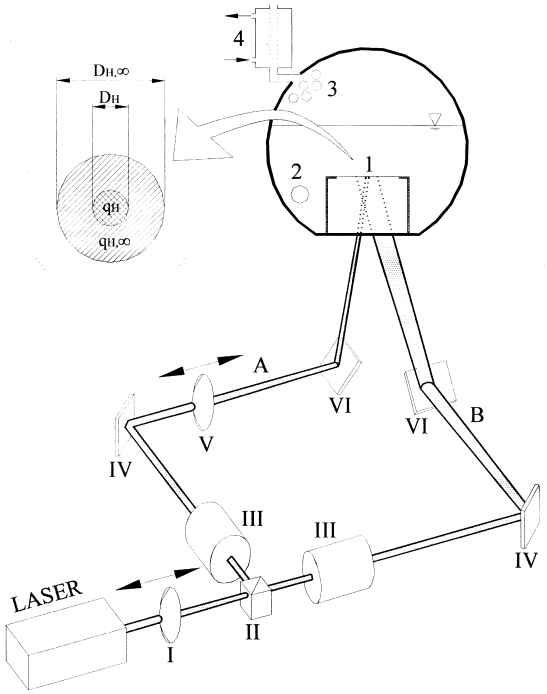

Fig. 1. Schematic diagram of the experimental set-up.

(IV) and (VI). Mirror (VI) redirected beams onto the metal foil, to the lower, "dry" part of the test section. The angles of the mirrors could be varied accurately around two axes using micrometer screws on the mirror mounts. By manually adjusting the angle of the mirrors, the angle of reflection of the laser beam was changed. In this manner it was possible to direct each beam to any spot on the lower part of the test section.

Fig. 1 shows that both beams travelled along the path described above, but that another lens (V) was placed in the path of beam (A) between mirrors (IV) and (VI), with an appropriate focal distance. By translatory movement of lenses (I) and (V), it was possible to separately set the diameters of beams (A) and (B). Laser beam (A) was used to heat a surface with a diameter D_H ranging from 1.66 to 5.3 mm with a heat flux q_H, while laser beam (B) heated the surrounding surface with a diameter $D_{H,\infty}$ ranging from 16 to 20 mm with a heat flux $q_{H,\infty}$, as can be seen in Fig. 1. If $q_{H,\infty} > 0$, the heat flux on the heating surface with a diameter D_H was the sum of both heat fluxes to this surface. A D_H greater than 5.3 mm was obtained by direct irradiation of the foil, without splitting the laser beam.

The power of beams (A) and (B) was set separately using two high-energy continuously variable attenuators (III). The attenuators had to be used because in normal regulation of the power supply unit the divergence of the laser beam changes with alterations to its power — with an increase in power, the laser beam diameter also increases. This problem was solved by using the attenuator which allows only the desired part of the beam energy to pass through while deflecting the rest of it without changing the beam geometry. The desired maximum power was set on the power supply unit and the attenuator was then used to change the power of the laser beam from zero to the preset maximum power. In this way it was possible to change the heat flux provided by an individual beam by changing only its power, while the heated surface area remained constant.

A photoelectric system was constructed to determine the diameter and position of the laser beams. Immediately below the test section where the laser beams hit, a silicon PIN photodiode with a very small active area, 0.56×0.56 mm, was installed on an XY translation stage, with a displacement accuracy of ± 4 μm. A photodiode changes the voltage of the output electrical current depending on its illumination. By changing the relative position of the photodiode with regard to the beam, the illumination of the photodiode changes, which is detected by measuring the output electrical voltage.

In determining the laser beam diameter D_H, the diameter at which the irradiance has fallen to 13.5% of the maximum values in the multi-mode operation was chosen. The beam diameter was determined on the basis of changes in the output voltage of the photodiode during its transverse movement across the laser beam, whereby the output voltage depends linearly on the illumination of the photodiode.

The experiments were conducted using copper and titanium foil with a thickness of 25 μm. In order to be able to determine the fraction of energy absorbed on the illuminated area of the foil, data on the diffusive reflectivity of the surface was needed. Measurements were performed using a Labsphere RSA PE-19 integration sphere on the same surfaces as were later used in the test section. The measured diffusive reflectivity for a clean copper surface at a wavelength of 1064 m was 98.4%, and for a clean titanium surface it was 59.7%. Because the fraction of absorbed energy for the copper is extremely small and in order to equalise the conditions, both foils were coated on one side with a 10–12 μm thick layer of highly temperature-resistant mat black paint in order to prevent problems resulting from reflected light. The mat black paint has a diffusive reflectivity of 5.4%, which means that the fraction of energy absorbed on the heated surface is 94.6%, $\mathscr{A} = 0.946$.

Heat flux can be calculated using equation

$$q_H = \frac{4}{\pi D_H^2} \mathscr{A} P \tag{1}$$

where P is the measured power of the laser beam before it reaches the test section and D_H is the measured beam diameter.

Water was degassed by boiling in the test vessel for at least two hours prior to the beginning of the experiment. The temperatures of the fluid and the vapour above it were measured with NiCr–Ni thermocouples. All tests were performed at atmospheric pressure 1.013 bar and at an average water temperature between 99°C and 100°C.

Prior to installation, the boiling side of the metal foil was cleaned with ethanol and rinsed with distilled water.

In order to determine the experimental uncertainties, we repeated a minimum of three times the experiment at each particular diameter of the heating area D_H. An error analysis of experimental uncertainty showed that the uncertainty in the q_{CHF} was within $\pm 9\%$, and for the smallest D_H it was within $\pm 15\%$. The uncertainty in the D_H was within $\pm 4\%$ and in the D_B/D_H it was within $\pm 13\%$.

The boiling experiments were recorded using a Sony Hi8 camcorder with a $48\times$ zoom and a speed of 25 full frames per second. The recording was digitised and transferred to a computer on which it was possible to split full frames into even and odd frames, which

yielded a succession of images with a temporal resolution of 20 ms.

3. Results

In agreement with Williamson and El Genk [19], we observed three different boiling modes on the small heating surfaces: (1) single bubbles; (2) growth of dual compartment bubbles which stabilise into prolate ellipsoids and then depart; and (3) which is the same as the previous mode except that the upper vapour portion is pinched off and departs, leaving a single bubble behind. On the basis of the conducted experiments it can be concluded that "vapour jets" resulting from vertical coalescence of several bubbles do not appear, because even at high heat fluxes no vertical coalescence was observed between more than two bubbles.

With larger heating surface diameters, the vapour mass behaviour at high heat flux boiling was similar to that observed in classical experiments of water boiling on horizontal electrically heated disk heaters, such as those with $D_H = 20$ mm [20], $D_H = 10$ mm [16] and with $D_H = 8$ mm [21]. At high heat flux boiling, vapour mushrooms consist of two different shapes of vapour masses, semicircular and cylindrical, which usually appear in pairs. At lower heat fluxes as well, one or two bubbles with a small diameter were formed immediately after the departure of a large bubble as a consequence of more favourable conditions for the growth of the next vapour mass, which is probably the result of pressure conditions behind the departing larger semicircular vapour mass [22].

If nucleation sites are referred to as places in which a larger vapour mass begins to be formed, which then creates a bubble or a vapour mushroom, it can be said that at small heating surface diameters, bubbles were formed only at one active nucleation site. When the heating surface diameter D_H was increased, a nucleation site appeared on the heating surface. With an increase in the heat flux q_H, this site displayed a more and more agitated motion on the heating surface until another active nucleation site appeared and, depending on the D_H and q_H, several other simultaneously active nucleation sites formed. In these cases, a lateral coalescence of the adjacent bubbles was also noticed, which caused the formation of large vapour masses. The vapour mushroom regime and CHF were clearly noticeable.

The minimum heating surface diameter D_H on which two or several simultaneously active nucleation sites were observed depended on the material of the heating surface and the heat flux. For the case of high heat flux water boiling the range of D_H for the Cu foil, in which the transition occurs from the range with a single active nucleation site into the range with two or several simultaneously active nucleation sites, is between 2.4 and 3.4 mm. For the Ti foil this range is shifted to larger values of D_H between 3.3 mm and 4.13 mm.

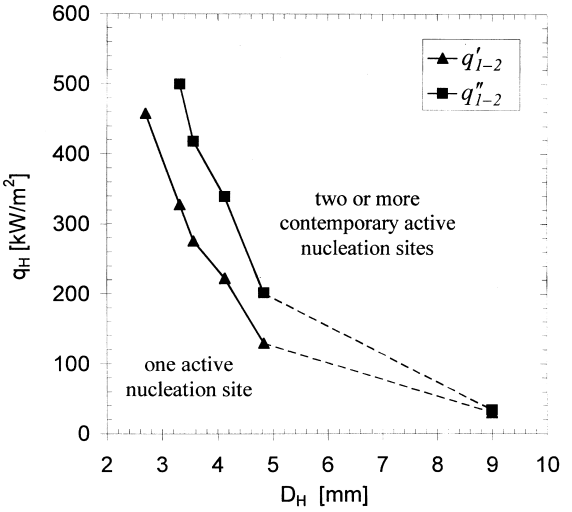

Fig. 2. The transition from boiling with one, to boiling with two or several simultaneously active nucleation sites on a 25 μm thick Cu foil.

For the case of water boiling on a Cu foil, Fig. 2 presents the upper and lower limit of the transition from the range with a single active nucleation site into the range, in which two or several nucleation sites are permanently active at the same time, depending on D_H and q_H.

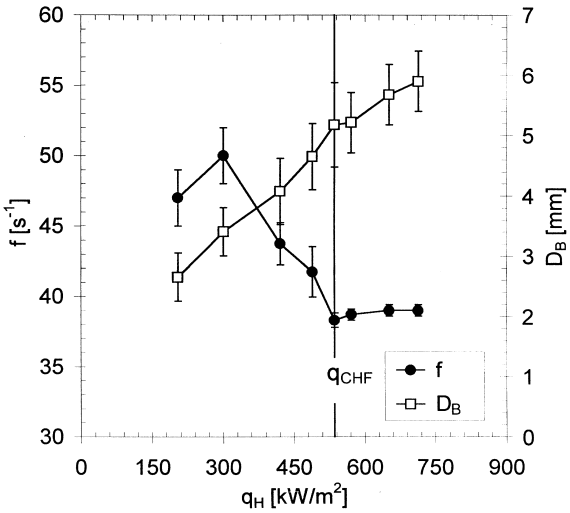

Fig. 3. The frequency and diameter of bubbles in boiling on a copper foil, $D_H = 3.58$ mm.

The lower limit of the transition range can be determined with the following equation

$$q'_{1-2} = 0.55917 D_H^{-2.3219} \quad (2)$$

with $R^2 = 0.9917$, while the upper limit of the transition range is

$$q''_{1-2} = 0.092754 D_H^{-2.7284} \quad (3)$$

with $R^2 = 0.9937$ with respect to measurements performed in the range 2.7 mm $< D_H <$ 9 mm. R^2 is the coefficient of determination, which is an indicator of how well the equation resulting from the regression analysis explains the relationship among variables.

3.1. Determination of critical heat flux

At high heat flux boiling, the bubble diameter increases considerably at CHF, while the frequency of bubble formation (vapour masses) is reduced to a minimum value and does not change significantly with further increases in q_H. Fig. 3 shows the variation of bubble formation frequency and their diameters on a copper heating surface with a diameter of $D_H = 3.58$ mm. The CHF is indicated with a vertical line.

At smaller diameters of the heating surface, $D_H < 2$ mm, it was not possible to determine CHF reliably using this method, because a sharp transition was not visible. The diameter and frequency of the bubbles changed by a small amount with increases in the heat flux and, above all frequency, with too large scatter to be able to reliably infer that CHF has occurred.

It is well known that, in addition to heat flux, the formation of nucleation sites is also influenced by the topography and material of the heating surface. In our case, the foil had a standard surface finish, as can be seen in Fig. 4a for the Cu foil with arithmetic mean

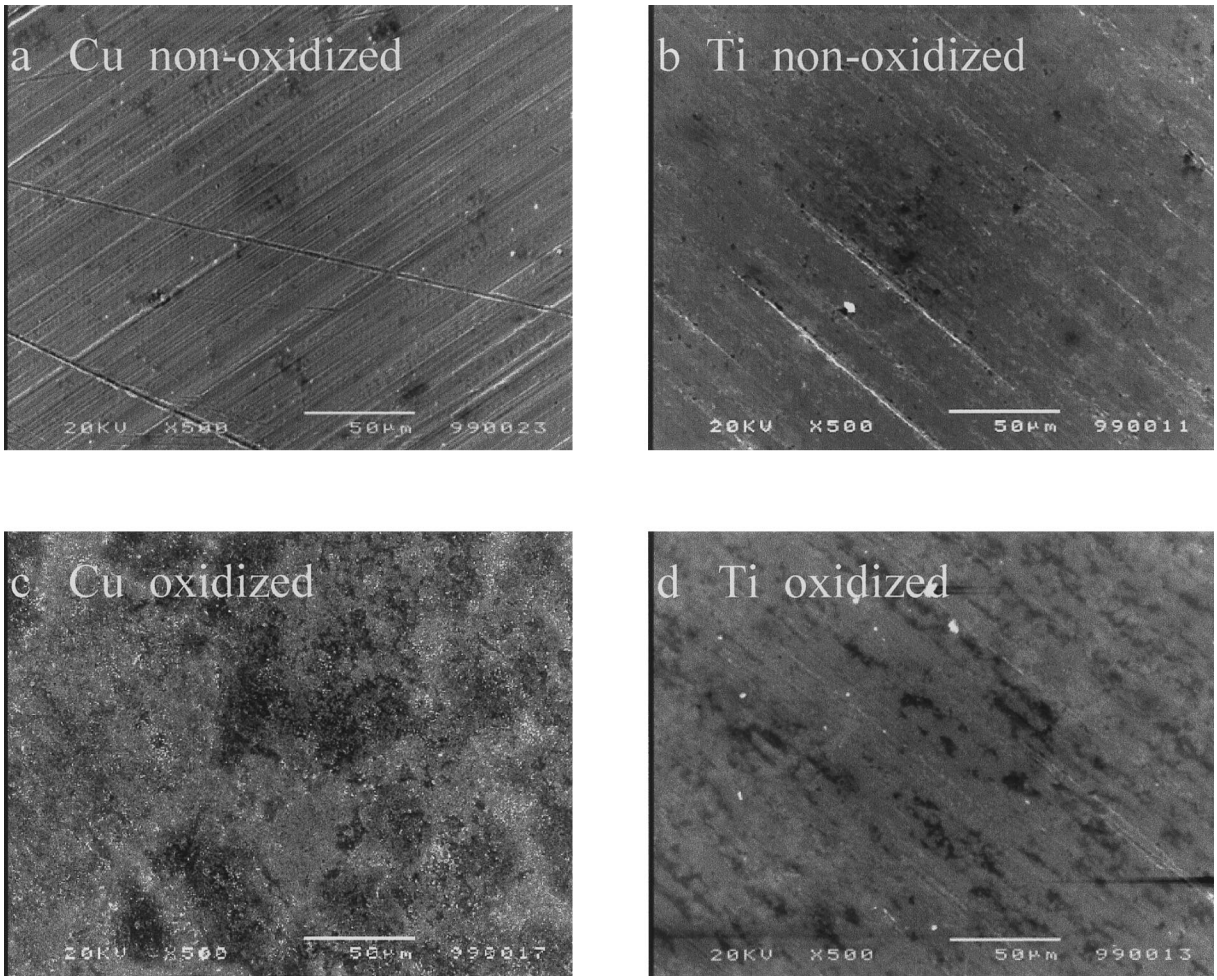

Fig. 4. Nonoxidised and oxidised Cu and Ti surfaces on a 25 μm foil at 500× magnification.

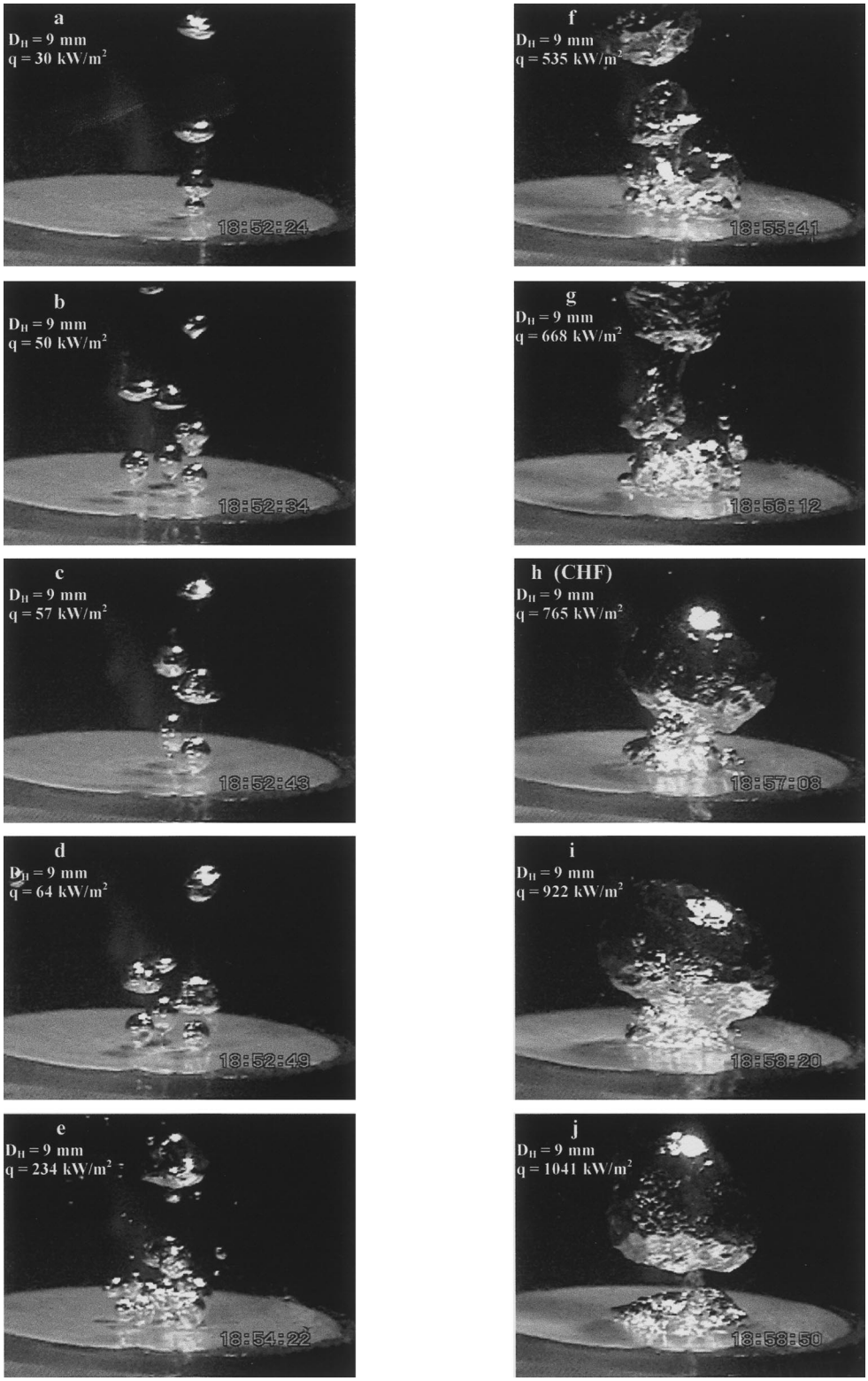

Fig. 5. Boiling on a laser-heated surface with a diameter of $D_H = 9$ mm on Cu foil at different heat fluxes.

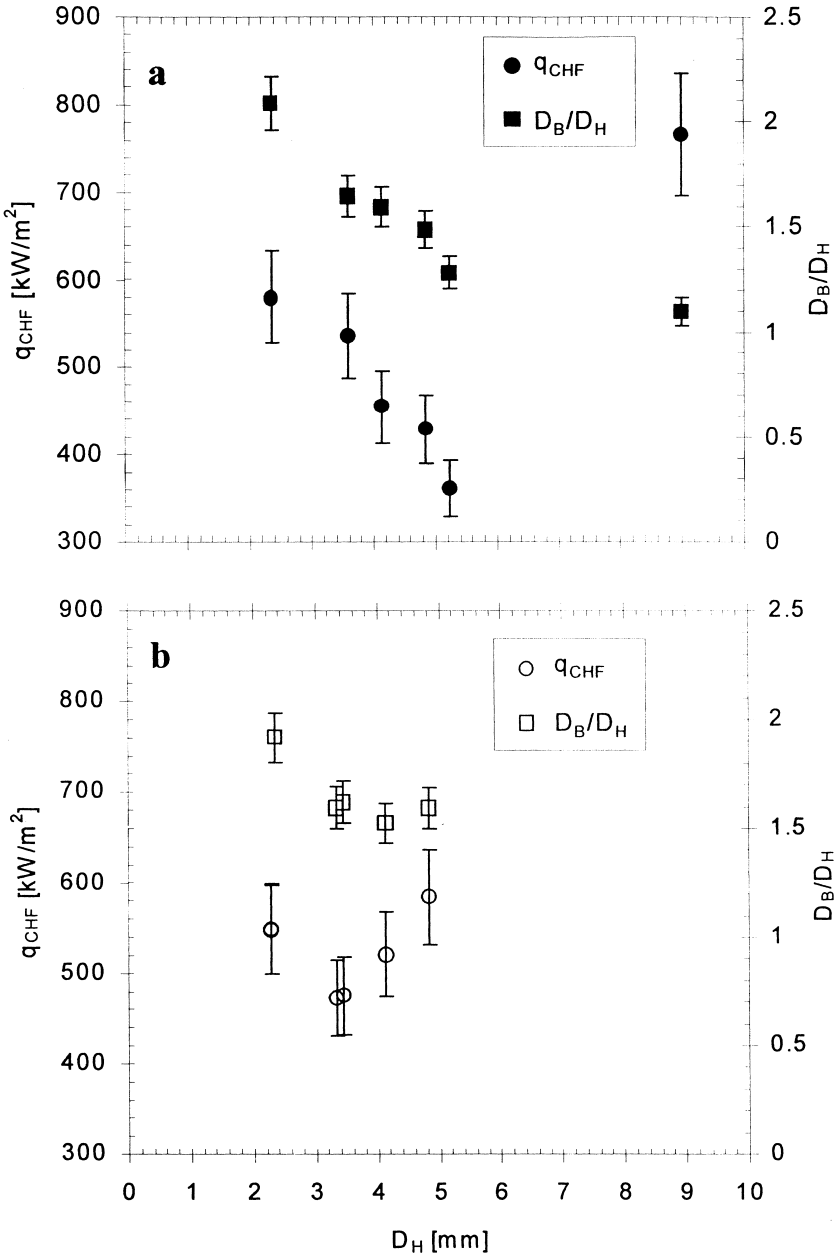

Fig. 6. q_{CHF} and D_B/D_H on Cu, **a**, and Ti, **b**, foil, versus diameter of the heated area D_H. The surrounding surface is not heated.

roughness $r_A = 0.17$ μm and Fig. 4b for the Ti foil with $r_A = 0.10$ μm. Surface roughness was measured with a Hommel Tester T2000.

In the film boiling range, burnout was achieved by further increasing q_H. At $D_H = 4.83$ mm and $q_H = 750$ W/m^2, a round oxidised layer with a diameter of 2 mm was created on the Ti foil, and at $D_H = 3.2$ mm and $q_H = 1.14$ MW/m^2, a burnout was detected. When Cu foil was used, a considerably higher heat flux was necessary at equal heating surface diameters for the surface to oxidise and be burned out. The reason for this can be found in a higher effusivity of Cu in comparison with Ti, $(\rho ck)^{0.5}_{Cu}/(\rho ck)^{0.5}_{Ti} = 6$ [8], therefore Cu transfers heat considerably better from an overheated spot to the surrounding surface. The oxidised surfaces are visible in Fig. 4c for the Cu foil and Fig. 4d for the Ti foil.

3.2. CHF and size of the heating surface

The study of the influence of the heating surface on CHF was performed by using only laser beam (A), with various diameter settings D_H, while the surrounding surface was not heated, $q_{H,\infty} = 0$.

The processes on the boiling surface depend on the heating surface diameter. During boiling on a surface with a diameter $D_H = 9$ mm on a Cu foil, which is shown in Fig. 5, the heating surface was sufficiently large for all types of boiling, from nucleation to film boiling, to be clearly visible. Fig. 5a–e show boiling at small heat flux. The heating surface is located in the middle of the foil. Nucleation began at 30 kW/m^2.

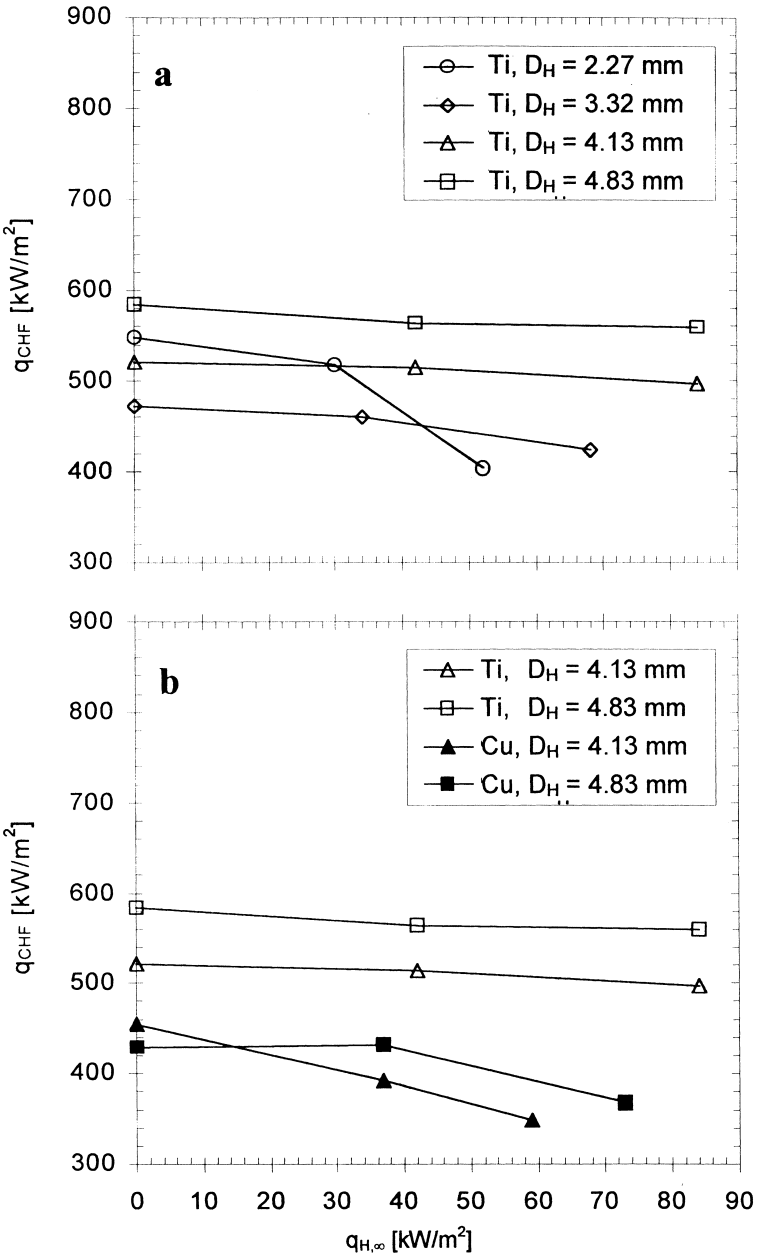

Fig. 7. The influence of heating of the surrounding surface $q_{H,\infty}$ on q_{CHF} at different heated surface diameters D_H on Ti, **a**, and on Ti and Cu, **b**, foil.

From 34 to 64 kW/m^2, two or three nucleation sites were active simultaneously, in alternation. With an increase in the heat flux, the size of the bubbles increased, Fig. 5f, and vapour masses began to appear due to their merging on the surface, Fig. 5g. CHF was achieved at 765 kW/m^2, Fig. 5h. A further rise in the heat flux increased the size of the vapour masses, Fig. 5i. At 1041 kW/m^2, a permanent vapour layer with a diameter of 10 mm was created on the heating surface, and the foil began to vibrate intensely, Fig. 5j. An oxidised circle with a diameter of 7.5 mm was created on the boiling surface.

The CHF and the ratio of the bubble/vapour mass diameter to the heating surface diameter, D_B/D_H versus the heating surface diameter D_H, are presented in Fig. 6a for the Cu foil and in Fig. 6b for the Ti foil. The minimum CHF achieved on the Cu foil was 361 kW/m^2 at $D_H = 5.23$ mm, and on the Ti foil it was 449 kW/m^2 at $D_H = 3.32$ mm.

With an increase in the heating surface diameter D_H, the ratio of the circumference to the area of the heating surface decreases. At large D_H, this ratio does not affect the CHF. For large heating surfaces, similar CHFs were measured as in the case of electric heating of thin ribbon heaters. The calculated value for a copper 25 μm ribbon heater is $q_{CHF} = 823$ kW/m^2 [8], while in our case $q_{CHF} = 765$ kW/m^2 was measured at $D_H = 9$ mm.

At small D_H, only one active nucleation site appeared, but an increase in D_H caused several such simultaneously active sites to appear. The CHF is influenced by parameters related to heat transfer to the heater, the heater-fluid interface and heat transfer from the heater to the fluid. In thin heaters, effusivity has a significant influence, as well as surface topography and surface chemistry, but these were not specifically analysed, because a standard foil was used. As can be seen in Fig. 6, the ratio of D_B/D_H has an important influence in small heating surfaces. Its variation with D_H is similar to that of the CHF. At small D_H, when only one nucleation site is active, CHF increases with a decrease in D_H. In addition, CHF increases with an increase in D_H from a certain particular value of D_H, which depends on the type of heating surface material. It follows from this that the CHF is significantly influenced by the number of simultaneously active nucleation sites.

3.3. CHF and surrounding surface heating

The difference between boiling on a laser-heated surface and boiling on an electrically heated surface is that in the first case a laser beam heats only a small circular segment of the surface. There is an area of contact between the heated and the surrounding surface, and its influence was analysed experimentally by heating the surrounding surface.

The positions of both laser beams (A) and (B) are shown in Fig. 1. CHF was determined for different diameters of the heating surface D_H on a Ti or Cu foil, whereby CHF was determined for each D_H at three different heat flux densities of the surrounding surface $q_{H,\infty}$.

Fig. 7a shows the variation of CHF with $q_{H,\infty}$ for various D_H on a Ti foil. For $D_H \geq 3.32$ mm, the variation of $q_{H,\infty}$ had no noticeable influence on CHF, while at $D_H = 2.27$ mm CHF decreased with an increase in $q_{H,\infty}$. At smaller diameters of the heating surface D_H, the conductance/capacitance effect increases with an increase in $q_{H,\infty}$. It is anticipated that at larger D_H the surroundings are no longer as intensely involved in the radial exchange of heat from the central part of the heated surface with a diameter of D_H.

Fig. 7b shows the influences of the boiling surface material and the diameter D_H on CHF with respect to $q_{H,\infty}$. With a decrease in D_H, a more intense influence of the heating of the surrounding surface can be observed on the Cu foil at larger diameters than on the Ti foil. For both presented D_H, CHF on the Ti foil is higher than that on the Cu foil.

The heat flux $q_{H,\infty}$ on the surrounding surface of the diameter $D_{H,\infty}$ was small. It was chosen in such a way that we went through the region of the onset of nucleation. The second points in Fig. 7a and b, with $q_{H,\infty} \approx 40$ kW/m^2, were just below the onset of nucleation. The third points, with $q_{H,\infty}$ from 52 to 85 kW/m^2, represent the conditions with the generation of bubbles of smaller intensity on the $D_{H,\infty}$, which did not have a significant influence on the CHF.

4. Conclusion

The technique of laser heating a thin metal foil enables experimental observation of local phenomena in pool boiling and CHF on a small flat heating surface.

The number of simultaneously active nucleation sites depends on the heat flux and the size and material of the heating surface. For the case of high heat flux water boiling, the ranges of the heating surface D_H for Cu and Ti foil were determined, in which the transition occurs from the range with a single active nucleation site into the range with two or several simultaneously active nucleation sites. For a 25 μm Cu foil with a standard surface finish, the transition between one and several simultaneously active nucleation sites was determined in a saturated pool boiling of water. At smaller diameters of the heating surface D_H, the limit

of this transition moves towards higher heat fluxes. CHF for smaller heating surfaces is lower than CHF on entirely heated surfaces. The variation of the ratio of bubble/vapour mass diameter to the heating surface diameter, D_B/D_H, with D_H is similar to that of CHF. CHF is significantly influenced by the number of simultaneously active nucleation sites. A more intense influence of heating the surrounding surface on CHF, which was observed at small D_H, is seen at higher D_H on the Cu foil than on the Ti foil.

The presented technique of laser heating a small flat boiling surface for the study of pool nucleate boiling and CHF is promising and will need to be upgraded by measuring the surface temperature with simultaneous accurate observation of the surface topography.

References

[1] J.H. Lienhard, V.K. Dhir, Hydrodynamic prediction of peak pool-boiling heat fluxes from finite bodies, ASME Journal of Heat Transfer 95 (1973) 152–158.

[2] F. Tachibana, M. Akiyama, H. Kawamura, Non-hydrodynamic aspects of pool boiling burnout, International Journal of Nuclear Science and Technology 4 (1967) 121–130.

[3] A. Bar-Cohen, A. McNeil, Parametric effects on pool boiling critical heat flux in dielectric liquids, in: Proceedings of Engineering Foundation Conference on Pool and External Flow Boiling, ASME, New York, 1992, pp. 171–175.

[4] A.A. Watwe, A. Bar-Cohen, The role of thickness and thermal effusivity in pool boiling CHF in highly-wetted liquids, in: Proceedings of the Tenth International Heat Transfer Conference, vol. 5, Taylor and Francis, Washington, DC, 1994, pp. 171–175.

[5] Y. Katto, Critical heat flux, International Journal of Multiphase Flow 20 (1994) 53–90.

[6] R.D.M. Carvalho, A.E. Bergles, The effects of the heater thermal conductance/capacitance on the pool boiling critical heat flux, in: Proceedings of Engineering Foundation Conference on Pool and External Flow Boiling, ASME, New York, 1992, pp. 203–211.

[7] I. Golobič, A.E. Bergles, Some aspects of heater-side factors on pool boiling critical heat flux, in: Proceedings of the First International Symposium on Two-Phase Flow Modelling and Experimentation, vol. 2, ETS, Pisa, 1995, pp. 873–879.

[8] I. Golobič, A.E. Bergles, Effects of heater-side factors on the saturated pool boiling critical heat flux, Experimental Thermal and Fluid Science 15 (1997) 43–51.

[9] P. Sadasivan, C. Unal, R.A. Nelson, Nonlinear aspects of high heat flux nucleate boiling heat transfer, ASME Journal of Heat Transfer 117 (1995) 981–989.

[10] D.B.R. Kenning, Y. Yan, Pool boiling heat transfer on a thin plate: features revealed by liquid crystal thermography, International Journal of Heat and Mass Transfer 39 (1996) 3117–3137.

[11] J. Hammer, P. Stephan, The role of micro-region phenomena on nucleate boiling heat transfer, in: Proceedings of the Second European Thermal Science Conference, vol. 1, ETS, Pisa, 1996, pp. 467–474.

[12] I. Golobič, E. Pavlovič, Computer model of nucleation site interactions on a thin plate, in: Proceedings of Engineering Foundation Conference on Convective Flow and Pool Boiling, Taylor and Francis, Washington, DC, 1999, pp. 119–124.

[13] R.A. Nelson, D.B.R. Kenning, M. Shoji, Nonlinear dynamics in boiling phenomena, Journal of Heat Transfer Society of Japan 35 (1996) 22–34.

[14] D. Gorenflo, A. Luke, E. Danger, Interactions between heat transfer and bubble formation in nucleate boiling, in: Proceedings of the Eleventh International Heat Transfer Conference, Kyongju, vol. 1, 1998, pp. 149–174.

[15] M. Shoji, Boiling chaos and modeling, in: Proceedings of the Eleventh International Heat Transfer Conference, Vol. 1., Kyongju, 1998, pp. 3–21.

[16] Y. Katto, S. Otokuni, Behavior of vapor masses on a vertical flat surface of comparatively large height near critical heat flux conditions in saturated pool boiling, International Journal of Heat and Mass Transfer 37 (1994) 255–263.

[17] S.G. Liter, M. Kaviany, CHF enhancement by modulated porous-layer coating, in: Proceedings of the ASME Heat Transfer Division, HTD-vol. 361-1, ASME, New York, 1998, pp. 165–173.

[18] H. Gjerkeš, I. Golobič, B. Gašperšič, Experimental study of interactions between spatially controlled nucleation sites on a thin flat plate in pool boiling, in: Proceedings of Engineering Foundation Conference on Convective Flow and Pool Boiling, Taylor and Francis, Washington, DC, 1999, pp. 111–117.

[19] C.R. Williamson, M.S. El-Genk, High-speed photographic analysis of saturated nucleate pool boiling at low heat flux, in: ASME Winter Meeting, Atlanta, 1991 91-WA-HT- 8, 7 p.

[20] R.F. Gaertner, Photographic study of nucleate pool boiling on a horizontal surface, ASME Journal of Heat Transfer 85 (1965) 17–29.

[21] C.-L. Yu, R.B. Mesler, A study of nucleate boiling near the peak heat flux through measurement of transient surface temperature, International Journal of Heat and Mass Transfer 20 (1977) 827–840.

[22] J. Mitrovič, Formation of a liquid jet after detachment of a vapour bubble, International Journal of Heat and Mass Transfer 40 (1997) 4309–4317.